Light induced modulation instability of surfaces under intense illumination

V. M. Burlakov, I. Foulds, and A. Goriely

Citation: Applied Physics Letters **103**, 251604 (2013); doi: 10.1063/1.4850532
View online: http://dx.doi.org/10.1063/1.4850532
View Table of Contents: http://scitation.aip.org/content/aip/journal/apl/103/25?ver=pdfcov
Published by the AIP Publishing

Light induced modulation instability of surfaces under intense illumination

V. M. Burlakov,[1,a)] I. Foulds,[2] and A. Goriely[1]
[1]*Mathematical Institute, University of Oxford, Woodstock Road, Oxford OX2 6GG, United Kingdom*
[2]*4700 King Abdullah University of Science and Technology, Thuwal 23955-6900, Kingdom of Saudi Arabia*

(Received 24 June 2013; accepted 2 December 2013; published online 17 December 2013)

We show that a flat surface of a polymer in rubber state illuminated with intense electromagnetic radiation is unstable with respect to periodic modulation. Initial periodic perturbation is amplified due to periodic thermal expansion of the material heated by radiation. Periodic heating is due to focusing-defocusing effects caused by the initial surface modulation. The surface modulation has a period longer than the excitation wavelength and does not require coherent light source. Therefore, it is not related to the well-known laser induced periodic structures on polymer surfaces but may contribute to their formation and to other phenomena of light-matter interaction.
 [http://dx.doi.org/10.1063/1.4850532]

Laser induced periodic structures on polymer surfaces (LIPSS) has attracted much attention in recent years because of their applications to micromechanics,[1–3] cell biology,[4,5] optics and photonics,[6] alignment of liquid crystals,[7] etc. There are two main categories of surface structures: (i) structures produced by material removal (ablation)[8,9] and (ii) structures formed due to redistribution of material with laser fluencies below ablation threshold.[10–16] A number of mechanisms have been proposed for LIPSS formation in the second category. All these mechanisms rely on spatial distribution of laser intensity over the surface produced either by appropriate focusing or passing the laser beam through a special mask,[17] or due to the interference of incident electromagnetic wave with the wave associated with surface vibrations,[18] scattered light,[19] or the waveguide mode(s).[10] Interference is usually invoked to explain periodicity of LIPSS and the fact that their period is close to the wavelength of incident light. Another observation explained by interference is that the surface structure wave vector in most cases is parallel to the polarization of the incident light.

Therefore, the main concept behind spontaneous (without phase or amplitude mask) LIPSS generation is light interference for which the coherence of incident radiation is essential. In this Letter, we show that there is an additional mechanism resulting in the formation of periodic surface modulation, which does not rely on interference effects. This mechanism that we call LIMIS (for Light Induced Modulation Instability of a Surface) is based on focusing and defocusing of homogeneous incident radiation beneath the modulated surface. Due to such redistribution of radiation energy, the material is heated inhomogeneously and expanded. In turn, this expansion provides a positive feedback to the initial surface modulation. Just like LIPSS,[20] LIMIS depends on light polarization as P-polarized light, for example, has higher transmission through slightly inclined surfaces than the S-polarized one. LIMIS also increases for shorter excitation wavelength and for materials with higher thermal expansion.

To describe this instability, we consider as an example a thin film of rubber polymer on a substrate kept at a constant temperature T_{subs}. The film is homogeneously illuminated with light and heated up above the glass transition temperature T_g by absorbing it. For simplicity, we assume that the film temperature is constant across the film. Then, the thermal expansion of the film results in an equilibrium thickness h(0) given by

$$h(0) = h_0[1 + \alpha \times (T - T_g)], \tag{1}$$

where h_0 is the film thickness at $T = T_g$, T is the film temperature, and α is thermal expansion coefficient of the polymer in rubber state.

Next, consider a small periodic perturbation of the film surface with amplitude Δ. This modulation forms a sequence of focusing and defocusing cylindrical lenses (in the 2D case) for the incident light. As a result, the light intensity is modulated inside the film and so is the temperature field. A generic relationship between the temperature and light intensity inside the film can be obtained from the heat balance taking into account heating by light and cooling due to heat drain to the substrate with temperature T_{subs}

$$\frac{\partial T}{\partial t} = \frac{1}{h_0 \rho C_P}\left[\gamma h_0 \bar{I}(x) - \eta_{\text{int}}(T - T_{subs})\right] + \frac{\eta}{\rho C_P}\frac{\partial^2 T}{\partial x^2}, \tag{2}$$

where $\bar{I}(x)$ is the average light intensity inside the film at lateral position x, γ is light absorption coefficient, η is the heat conductivity coefficient, η_{int} is the heat conductance through the film-substrate interface, C_P is specific heat capacity of the film material, and ρ is the material density. Here, we used an approximation of homogeneous heating through the film thickness due to weak light absorption and relatively quick thermal equilibration across the film. The product ρh_0 is the amount of material per unit area.

To obtain the distribution of light intensity inside the film, we assume that the film surface is sinusoidally modulated such that $h(x) = h(0) + \Delta \sin(kx)$, $\Delta \ll h(0)$, where k and Δ are the modulation wave vector and amplitude,

a)Author to whom correspondence should be addressed. Electronic mail: burlakov@maths.ox.ac.uk.

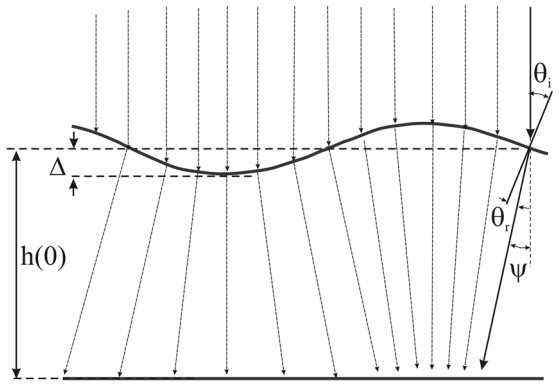

FIG. 1. Schematics of the light focusing-defocusing beneath the polymer surface (thick solid curve) sinusoidally modulated with the amplitude Δ. θ_i, θ_t, and ψ are the local angles of incidence, refraction, and light beam deviation, respectively, h(0) is the equilibrium film thickness before spontaneous modulation.

respectively. If the angle of light incidence on the surface with respect to the normal is small and equal to θ_i then the refracted angle is $\theta_r = \theta_i/n_2$, where n_2 is refractive index of the material. We are interested in the angle of the light beam deviation from its direction of incidence ψ (see Fig. 1). Using the approximation $\theta_i \approx dh(x)/dx$, this angle can be expressed as $\psi(x) = \left(\frac{n_2-1}{n_2}\right)\frac{dh(x)}{dx}$. The position of the light beam x_1 at a distance y from the film surface is

$$x_1 = x + y\psi(x) = x + y\left(\frac{n_2-1}{n_2}\right)\frac{dh(x)}{dx}. \tag{3}$$

The light intensity $I(x_1, y)$ is proportional to the density of beams $(dx_1/dx)^{-1}$, so that

$$I(x_1,y) \approx I(x,y) \approx I_0 \times (1-R_0)(1-\gamma y) \times \left(1 + yk^2\Delta\left(\frac{n_2-1}{n_2}\right)\sin(kx)\right), \tag{4}$$

where I_0 is the incident light intensity, I_0 is reflectivity of a flat surface and we assumed weak light absorption $\gamma y \ll 1$ and neglected higher order terms in Δ. Equation (4) shows that the light intensity is increased under the surface where $d^2h(x)/dx^2 < 0$ indicating focusing effect of the convex half-period of surface modulation, and it is decreased beneath the concave half-period $\left(d^2h(x)/dx^2 > 0\right)$ due to the defocusing effect. It also demonstrates that the intensity modulation increases with increasing k. As upon increase, k becomes compatible with the light wave vector k_L the modulation intensity decreases due to diffraction effects, as illustrated below.

The above analysis is based entirely on geometric optics. Therefore, it does not consider light diffraction on the periodic surface structure. The latter can be represented as a linear array of alternating cylindrical focusing and defocusing lenses. Diffraction increases when the array period decreases becoming compatible with the incident light wavelength. As the lateral distribution of the film temperature is due to light absorption throughout the film, diffraction effects have to be averaged over the film thickness. The impact of this averaged diffraction at onset (that is when Fresnel number $N_F = l^2/(\lambda_L y) > 1$, where λ_L is the wavelength of light[21]) is to smear off the light intensity distribution calculated within the geometric optics approximation. The effect of smearing can be modelled by a convolution of the function given by Eq. (4) by a weight function $f(x)$ $\left(\int f(x)dx = 1\right)$. For illustration purposes, the function $f(x)$ is chosen to be equal to $k_L/(yk)$ for $-y\frac{k}{2k_L} < x < y\frac{k}{2k_L}$ $(k_L = 2\pi/\lambda_L)$ and zero otherwise. Thus, $f(x)$ has an effective width roughly corresponding to half width of the far-field (Frounhofer) diffraction function.[22] The light intensity distribution averaged over the film thickness $\bar{I}(x)$ then takes the form

$$\bar{I}(x) \approx I_0 \times (1-R_0)\left(1 - \frac{1}{2}\gamma h(0)\right) + 4I_0\frac{(1-R_0)k_L^2\Delta}{k^2h(0)} \times \left(\frac{n_2-1}{n_2}\right)\sin(kx)\left(1 - \cos\left(\frac{k^2h(0)}{2k_L}\right)\right). \tag{5}$$

Since the shear moduls of polymers in rubber state (above glass transition temperature) is very low,[23] we assume that the surface modulation is entirely due to lateral temperature variation in the film. Expressing therefore T from Eq. (1) with h(0) replaced by $h(x) = h(0) + \Delta\sin(kx)$ and substituting the result into Eq. (2), we obtain

$$\frac{\sin(kx)}{\alpha h_0}\frac{d\Delta}{dt} = \frac{\gamma h_0 I_0(1-R_0)}{h_0\rho C_P}\left(\left(1 - \frac{1}{2}\gamma h(0)\right) + \frac{4k_L^2\Delta}{k^2h(0)}\left(\frac{n_2-1}{n_2}\right)\sin(kx)\left(1 - \cos\left(\frac{k^2h(0)}{2k_L}\right)\right)\right) + \frac{1}{h_0\rho C_P}\left[-\eta_{\text{int}} \times \left(\frac{h(0) + \Delta\sin(kx) - h_0}{\alpha h_0} + T_g - T_{subs}\right)\right] - \sin(kx)\frac{k^2\eta\Delta}{\rho C_P\alpha h_0}. \tag{6}$$

Eliminating the part associated with the flat surface $\gamma I_0(1-R_0) \times \left(1 - \frac{1}{2}\gamma h(0)\right) - \frac{\eta_{\text{int}}}{h_0}\left(\frac{h(0)-h_0}{\alpha h_0} + T_g - T_{subs}\right) = 0$ and assuming in the rest $h(0) \approx h_0$ (the film temperature is slightly above T_g), we obtain the main equation describing time evolution of the perturbation amplitude $\frac{d\Delta}{dt} = \beta\Delta$, where

$$\beta = \frac{1}{\rho C_P}\left[\frac{4\alpha\gamma I_0(1-R_0)k_L^2}{k^2}\left(\frac{n_2-1}{n_2}\right) \times \left(1 - \cos\left(\frac{k^2h_0}{2k_L}\right)\right) - k^2\eta - \frac{\eta_{\text{int}}}{h_0}\right]. \tag{7}$$

According to this equation the surface perturbation grows if $\beta > 0$. The first term in brackets of Eq. (7) determines the

amplitude of light intensity modulation inside the material due to surface modulation. If the material thermal conductance η and interface conductance η_{int} are low and the thermal expansion is high enough then the modulation of light intensity produces a positive feedback to the surface modulation increasing its amplitude.

The growth rate β for the surface modulation calculated using Eq. (7) and the material parameters of polystyrene is shown in Fig. 2. According to this figure, surface modulation instability ($\beta > 0$) exists in a certain range of modulation wave vectors and this range increases with decreasing incident light wavelength. The onset for surface modulation at low k values is due to heat conduction, which smears off the effect of thermal expansion along the film surface. The offset of instability at larger k is due to diffraction, which smears off the distribution of light intensity hence that of temperature inside the film. Fig. 3 gives the light intensity threshold for different excitation wavelength. If all other parameters are kept constant, then for shorter excitation wavelength the power density required to initiate surface instability is lower. Curve 3 in Fig. 3 illustrates the role of the thermal expansion coefficient: high thermal expansion coefficients lead to a stronger positive feedback by the modulated light intensity inside the film hence lowering the intensity threshold.

This linear stability analysis applies to a superposition of surface modulations and results in the growth of surface roughness. We believe therefore that there are two mechanisms working in parallel that are responsible for the formation of LIPSS: at the early stages of illumination there is an increase of surface roughness due to LIMIS effect. Simultaneously and at later stages, the light scattered on the increasingly rougher surface interferes with the incident light selecting a continuing narrow spectrum of roughness spatial harmonics, which grows further and eventually results in LIPSS formation. This sequence of events though interpreted differently has been observed experimentally in Ref. 14.

In practice, LIPSS are usually generated with pulsed laser excitation; therefore, it is important to check how the conditions of LIMIS depend on the laser pulse parameters. Following the ideas of Ref. 25, we write a generic equation

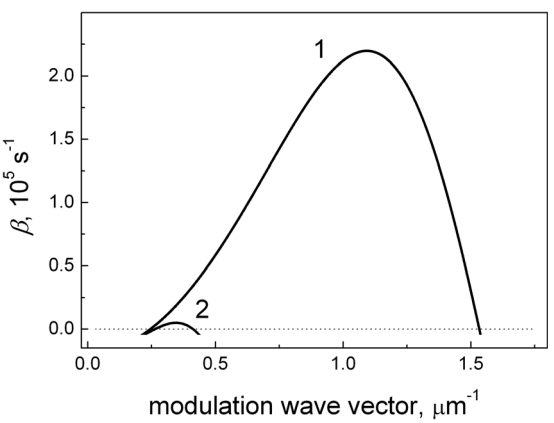

FIG. 2. Growth rate β of the periodic surface structure (see Eq. (7)) as a function of its wave vector k for two excitation light wave-lengths 1—$\lambda_L = 10.6\mu$ (CO_2 laser) and 2—$\lambda_L = 1.06\mu$ (YAG:Nd^{3+} laser). The model parameters are: $I_0 = 1.5\,\text{kW/cm}^2$, $\alpha = 0.05$, $\gamma = 0.01\,\mu\text{m}^{-1}$, $h_0 = 20\,\mu\text{m}$, $n_2 = 1.57$,[24] $\eta = 10^{-7}\,\text{W}\mu\text{m}^{-1}\text{K}^{-1}$, $\eta_{\text{int}} = 2\times10^{-7}\,\text{W}\,\mu\text{m}^{-2}\text{K}^{-1}$, ρ=1.06 $\times10^{-12}\,\text{g}\mu\text{m}^{-3}$, and $C_p = 1.25\,\text{Jg}^{-1}\text{K}^{-1}$.

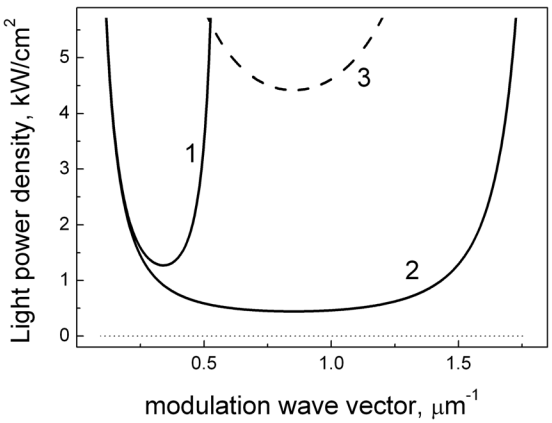

FIG. 3. Light intensity I_0 required for triggering surface modulation instability as a function of the modulation wave vector for two excitation wavelength 1—$\lambda_L = 10.6\mu$ (CO_2 laser) and 2—$\lambda_L = 1.06\mu$ (YAG:Nd^{3+} laser). Other parameter values are given in caption to Fig. 2. Curve 3 was calculated for $\alpha = 0.005$ and $\lambda_L = 1.06\mu$ to illustrate the role of thermal expansion coefficient.

of energy balance taking into account finite rate of heat transport

$$\frac{\partial Q(x,t)}{\partial t} = \gamma I(x,t) + \eta\frac{\partial^2 T(x,t-\tau)}{\partial x^2}. \tag{8}$$

Note that the last term in the RHS implies that all the derivatives of temperature should be taken at earlier time $t-\tau$, where τ is the characteristic delay time for heat diffusion. We are interested in a situation where the film is under the action of a laser pulse and all relevant phenomena, such as the modulation instability, take place within the pulse duration t_P. Assuming that the surface modulation is a simple harmonic (see Fig. 1) and its amplitude is a relatively slow function of time on the time scale of t_P we may rewrite Eq. (8) as $\rho C_P\frac{\partial T(x,t)}{\partial t} = \gamma I(x,t) + \eta F(t_P/\tau)\frac{\partial^2 T(x,t)}{\partial x^2}$. Here, we transferred the effect of the delayed change in temperature gradients to the delayed change in the heat conductivity of the film material accounted by the function $F(t_P/\tau)$. The latter should apparently fulfil the conditions $F(t_P/\tau) = 0$ if $t_P \ll \tau$ and $F(t_P/\tau) = 1$ if $t_P \gg \tau$. For illustration purposes, we use the following form of his function $F(t_P-\tau) = 1 - \exp\left[-(t_P/\tau)^2\right]$. Repeating the above analysis of surface modulation instability with the heat conductivities multiplied by the factor $F(t_P/\tau)$, we obtain the following expression in place of Eq. (7):

$$\beta = \frac{1}{\rho C_P}\left[\frac{4\alpha\gamma I_0(1-R_0)k_L^2}{k^2}\left(\frac{n_2-1}{n_2}\right)\times\left(1-\cos\left(\frac{k^2h_0}{2k_L}\right)\right) - k^2\eta F(t_P/\tau)\right], \tag{9}$$

where for simplicity we neglected the unknown heat transport through the film-substrate interface. For illustrating the effect of laser pulse on LIMIS, Eq. (9) was implemented to the experimental conditions described in Ref. 26 with the parameters of laser excitation and the material (PET) summarized in Table I. The length scale for the lateral heat transport

TABLE I. Characteristics of laser pulse excitation: central wavelength λ_L, pulse duration t_P, light power density I_0 during the pulse, and material parameters of polyethylene terephthalate PET: refractive index n_2, absorption coefficient γ, characteristic delay time τ, specific density ρ, specific heat capacity C_P, heat conductivity η, and thermal expansion coefficient α.

Excitation wavelength/excitation and material parameters	$\lambda_L = 265$ nm	$\lambda_L = 795$ nm
t_P, fs	260	120
I_0, W/cm^2	7.7×10^5	6×10^6
n_2	1.7	1.6
γ, cm^{-1}	2×10^4	4×10^2
τ, s	0.265×10^{-9}	0.795×10^{-9}
ρ, g/cm^3	1.37	1.37
C_P, J/g/K	1.0	1.0
η, J/m/K	0.15	0.15
α	7×10^{-5}	7×10^{-5}

in this case is λ_L, which gives a value for $\tau = \lambda_L/v_S$, where $v_S = 10^5$ cm/s is the sound velocity in the polymer.

The growth rate as a function of the wave vector is shown in Fig. 4. According to this figure, the growth rate maximum corresponds to the surface structure wave vector higher than that of the incident light. This means that at least in the beginning of structure formation its period is shorter than the incident light wavelength, as observed experimentally.[26] One can see also that the maximum growth rate for $\lambda_L = 795$ nm is lower by a factor 20 than that for $\lambda_L = 265$ nm. Assuming that the surface structure amplitude is proportional to the growth rate, we may conclude surface structure generation with $\lambda_L = 795$ nm requires about 20 times higher fluence than that with $\lambda_L = 265$ nm, which is also consistent with available experimental data.[26]

It is worth pointing out that LIMIS with pulsed excitation as illustrated in Fig. 4 is quite high even for relatively high heat conductance and low thermal expansion. This is due to the delay in heat transport relative to thermal expansion, as the latter is instantaneous and follows the light intensity while the former needs some time to develop. Equation (9) also gives the dependence of the growth rate at $k = k_L$ on

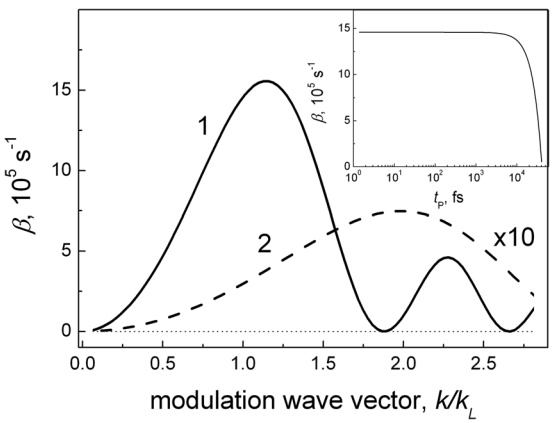

FIG. 4. Growth rate β of the periodic surface structure (see Eq. (9)) as a function of its wave vector k for two excitation light wave-lengths 1—$\lambda_L = 265$ nm and 2—$\lambda_L = 795$nm. All other parameters are given in Table I. Inset shows the dependence of the growth rate for $\lambda_L = 265$ nm at $k = k_L$ on the pulse duration t_P.

t_P with all the other parameters kept constant–see inset in Fig. 4. According to this figure, the instability disappears if the laser pulse is too long, i.e., when heat transport has enough time to smear off the thermal expansion. Note that the offset pulse duration for β seen in the inset in Fig. 4 may not correspond to a physically attainable value due to the qualitative character of the function $F(t_P/\tau)$ and the use of the heat conductivity and thermal expansion coefficient measured at much lower (room) temperature than the one attained during the laser pulse.

So far we have neglected the incident light polarization, i.e., the fact that induced one-dimensional modulation of irradiated surface may have preferential orientation with respect to polarization of the incident light. To check the polarization dependence of $R_S \approx R_0\left(1 + \frac{\Delta^2 k^2}{n_2}\right)$ and $R_P \approx R_0\left(1 - \frac{\Delta^2 k^2}{n_2+1}\right)$, where the subscripts S and P stand for S- and P-polarization, respectively. Replacing R_0 in Eq. (7) with both R_S and R_P and comparing the corresponding threshold intensities, we find that $I_{0S} > I_{0P}$, i.e., the surface modulation develops faster in the direction parallel to the incident light polarization than in the perpendicular direction.

In conclusion, we have described a mechanism leading to surface modulation instability of a plastic material under intense illumination by coherent or non-coherent radiation. The mechanism involves two main phenomena: (i) the focusing and defocusing of radiation by sinusoidally modulated surface, which generates sinusoidal modulation of radiation intensity inside the material; (ii) the local thermal expansion of the material due to the radiation intensity which further increases initial surface modulation thus providing a positive feedback. As the material flow has not been considered in our approach, the effect of LIMIS is reversible: it disappears after the light is switched off. It is, however, expected that irreversible plastic flow during irradiation would freeze most of the generated pattern. The modulation instability can also greatly enhance the efficiency of mechanisms involving light scattering on surface roughness. LIMIS is mostly relevant for materials with high thermal expansion and low elastic modulus. Most materials have rather low thermal expansion coefficients ($<0.001\,\mathrm{K}^{-1}$); therefore, the threshold intensity for the modulation instability could be much higher for them than the breakdown threshold under continuous illumination, but can be realized under moderate illumination intensity if pulsed illumination with sufficiently short pulses is used. In a continuous illumination regime, LIMIS is most relevant for rubber polymers, which may have thermal expansion coefficients as high as 0.05. This makes them very prone to developing surface modulation especially under shorter excitation wavelength. Further theoretical and experimental studies are required to clarify the role of the modulation instability in LIPSS generation and to find out the properties of the steady state surface structures developing due to LIMIS taking into account the flow of illuminated material.

This publication was based on work supported in part by Award No. KUK C1-013-04, made by King Abdullah University of Science and Technology (KAUST). A.G. is a Wolfson/Royal Society Merit Award Holder and acknowledges support from a Reintegration Grant under EC

Framework VII. We also benefited from early discussion with Jon Chapman, Peter Stewart, and Matt Hennessy.

[1]M. Bolle and S. Lazare, Appl. Surf. Sci. **65–66**, 349 (1993).
[2]M. Bolle and S. Lazare, Appl. Surf. Sci. **69**, 31 (1993).
[3]P. Slepicka, E. Rebollar, J. Heitz, and V. Svorcik, Appl. Surf. Sci. **254**, 3585 (2008); S.-H. Lee, C.-W. Yang, and J.-W. Park, Surf. Coat. Technol. **207**, 24 (2012).
[4]E. Rebollar, I. Frischauf, M. Olbrich, T. Peterbauer, S. Hering, J. Preiner, P. Hinterdorfer, C. Romanin, and J. Heitz, J. Biomater. **29**, 1796 (2008).
[5]M. Schernthaner, B. Reisinger, H. Wolinski, S. D. Kohlwein, A. Trantina-Yates, M. Fahrner, C. Romanin, H. Itani, D. Stifter, G. Leitinger, K. Groschner, and J. Heitz, Acta Biomater. **8**, 2953 (2012).
[6]M. Castillejo, T. A. Ezquerra, M. Martín, M. Oujja, S. Pérez, and E. Rebollar, AIP Conf. Proc. **1464**, 372 (2012); K. O. Hill, Y. Fujii, D. C. Johnson, and B. S. Kawasaki, Appl. Phys. Lett. **32**, 647 (1978).
[7]C. J. Newsome, M. O'Neill, R. J. Farley, and G. P. Bryan-Brown, Appl. Phys. Lett. **72**, 2078 (1998).
[8]T. Lippert, T. Gerber, and A. Wokaun, Appl. Phys. Lett. **75**, 1018 (1999).
[9]J. Reif, F. Costache, M. Henyk, and S. V. Pandelov, Appl. Surf. Sci. **197–198**, 891 (2002).
[10]H. Hiraoka and M. Sendova, Appl. Phys. Lett. **64**, 563 (1994).
[11]M. Bolle, S. Lazare, M. Le Blanc, and A. Wilmes, Appl. Phys. Lett. **60**, 674 (1992).
[12]M. Csete, S. Hild, A. Plett, P. Zlemann, Zs. Bor, and O. Marti, Thin Solid Films **453**, 114 (2004).
[13]M. Li, Q. H. Lu, J. Yin, Y. Sui, G. Li, Y. Qian, and Z. G. Wang, Appl. Surf. Sci. **193**, 46 (2002).
[14]M. Csete and Z. Bor, Appl. Surf. Sci. **133**, 5 (1998).
[15]M. Csete, R. Eberle, M. Pietralla, O. Marti, and Z. Bor, Appl. Surf. Sci. **208–209**, 474 (2003).
[16]S. Lazare and P. Benet, Appl. Phys. **74**, 4953 (1993).
[17]I. Apostol, V. Damian, P. C. Logofatu, D. Apostol, I. Iordache, and R. Muller, Romanian Reports in Physics **63**, 172 (2011).
[18]A. M. Bonch-Bruevich, M. N. Libenson, V. S. Makin, and V. Trubaev, Opt. Eng. **31**, 718 (1992).
[19]J. E. Sipe, J. F. Young, J. S. Preston, and H. M. van Driel, Phys. Rev. **27**, 1141 (1983).
[20]B. Tan and K. Venkatakrishnan, J. Micromech. Microeng. **16**, 1080 (2006).
[21]M. Born and E. Wolf, *Principles of Optics* (Cambridge University Press, Cambridge, 1999).
[22]E. Hecht, *Optics* (Addison-Wesley, 2002), Figures 10.6(b) and 10.7(e).
[23]G. Gee, Contemp. Phys. **11**, 313 (1970); J. C. Loettersy, W. Olthuis, P. H. Veltink, and P. Bergveld, J. Micromech. Microeng. **7**, 145 (1997).
[24]S. N. Kasarova, N. G. Sultanova, C. D. Ivanov, and I. D. Nikolov, Opt. Mater. **29**, 1481 (2007).
[25]E. Marin, J. Marin, and R. Hechavarria, Journal de Physique IV **125**, 365 (2005).
[26]E. Rebollar, J. R. V. de Aldana, J. A. Pérez-Hernández, T. A. Ezquerra, P. Moreno, and M. Castillejo, Appl. Phys. Lett. **100**, 041106 (2012).